



1 **Freshening of Antarctic Intermediate Water in the South Atlantic Ocean in 2005 - 2014**

2 Wenjun Yao¹, Jiuxin Shi¹

3 ¹Key Lab of Physical Oceanography (Ocean University of China), Ministry of Education,
4 Qingdao 266100, Shandong, China

5 *Correspondence to:* E-mail address: wjimiao@gmail.com (Wenjun Yao)

6 **Abstract**

7 Basin-scaled freshening of Antarctic Intermediate Water (AAIW) is reported to have
8 dominated South Atlantic Ocean during period from 2005 to 2014, as shown by the gridded
9 monthly means Argo (Array for Real-time Geostrophic Oceanography) data. The relevant
10 investigation was also revealed by two transatlantic occupations of repeated section along 30 °
11 S, from World Ocean Circulation Experiment Hydrographic Program. Freshening of the
12 AAIW was compensated by the opposing salinity increase of thermocline water, indicating
13 the contemporaneous hydrological cycle intensification. This was illustrated by the
14 precipitation less evaporation change in the Southern Hemisphere from 2000 to 2014, with
15 freshwater input from atmosphere to ocean surface increasing in the subpolar
16 high-precipitation region and vice versa in the subtropical high-evaporation region. Against
17 the background of hydrological cycle augment, the decreased transport of Agulhas Leakage
18 (AL) was proposed to be one of the contributors for the associated freshening of AAIW. This
19 indirectly estimated variability of AL, reflected by the weakening of wind stress over the
20 South Indian Ocean since the beginning of 2000s, facilitates the freshwater input from source
21 region and partly contributes to the observed freshened AAIW. Both of our mechanical
22 analysis is qualitative, but this work would be helpful to validate and test predictably coupled
23 sea-air model simulations.

24 **Keywords:** Freshening; Antarctic Intermediate Water; South Atlantic; Agulhas Leakage;
25 Wind Stress

26 **1. Introduction**

27 Thermocline and intermediate waters play an important role on global overturning
28 circulation by ventilating the subtropical gyres in different parts of the world oceans [*Sloyan*



29 *and Rintoul, 2001*]. Meanwhile they also constitute the northern limb of the Southern
30 Hemisphere supergyre [*Ridgway and Dunn, 2007; Speich et al., 2002*].

31 Many studies have focused on the variability of intermediate water. *Wong et al.* [2001]
32 pointed out that the intermediate water had freshened from 1960s to 1985-94 in the Pacific
33 Ocean, *Bindoff and McDougall* [2000] reported that there had been freshening of water
34 between 500 and 1500 db from 1962 to 1987 along 32 °S in the Indian Ocean, and *Curry et al.*
35 [2003] discovered the salinity reduction on the isopycnal surface of intermediate water for the
36 period 1950s - 1990s in the western Atlantic. All of the freshening variability can be traced
37 back to the signature of water in the formation regions [*Church et al., 1991*]. The freshening
38 above are in agreement with the worldwide augment of hydrological cycle, in which context
39 the wet (precipitation > evaporation, $P > E$ dominance) subpolar regions have been getting
40 wetter and vice versa for the dry ($P < E$ dominance) subtropical regions since the last 50 years
41 [*Held and Soden, 2006; Skliris et al., 2014*].

42 Antarctic Intermediate Water (AAIW) is characterized by salinity minimum (core of
43 AAIW) and concentrated at depth 600 - 1000 m (Fig. 1), lies within potential density
44 (reference to sea surface) $\sigma_{\theta} = 27.1 - 27.3 \text{ kg/m}^3$ [*Piola and Georgi, 1982*]. The AAIW is
45 found from just north of the Subantarctic Front (SAF) [*Orsi et al., 1995*] in the Southern
46 Ocean and can be traced into as far as 20 °N [*Talley, 1996*]. It is generally accepted that the
47 variability of AAIW is largely controlled by air-sea-ice interaction [*Close et al., 2013;*
48 *Naveira Garabato et al., 2009; Santoso and England, 2004*], but the argument about its origin
49 and formation process is still going on. The first popular one is the controversially
50 circumpolar formation theory of AAIW along SAF, through mixing with Antarctic Surface
51 Water (AASW) along isopycnal [*Fetter et al., 2010; Sverdrup et al., 1942*]. And the other is
52 the local formation perspective of AAIW in specific regions, as bi-product of Subantarctic
53 Mode Water (SAMW) relating to deep convection [*McCartney, 1982; Piola and Georgi,*
54 1982].

55 In the South Atlantic, AAIW constitutes the return branch of the Meridional Overturning
56 Circulation (MOC) [*Donners and Drijfhout, 2004; Speich et al., 2007; Talley, 2013*]. As an
57 open ocean basin, South Atlantic is fed by two different AAIW [*Sun and Watts, 2002*]. The



58 first is the younger, fresher and lower apparent oxygen utilization (AOU) AAIW originated
59 from the Southeast Pacific [McCartney, 1977; Talley, 1996] and the winter waters west of
60 Antarctic Peninsula [Naveira Garabato *et al.*, 2009; Santoso and England, 2004]. Almost all
61 these origin regions of AAIW is dominated by the net surface freshwater flux from
62 atmosphere to ocean ($P>E$), which facilitates the freshening of AAIW with time. The second
63 is the older, saltier and higher AOU AAIW comes from Indian Ocean, transported by Agulhas
64 Leakage (AL) as Agulhas rings (Fig. 2). The mixture of the above two types of AAIW can
65 lead to transition for hydrographic properties across the subtropical South Atlantic [Boebel *et*
66 *al.*, 1997].

67 The influence of AL on variability of AAIW in the South Atlantic has been
68 demonstrated to be greatly large [Hummels *et al.*, 2015; Schmidtko and Johnson, 2012], as 50
69 - 60% of the Atlantic AAIW originates from the Indian Ocean [Gordon *et al.*, 1992; G D
70 McCarthy *et al.*, 2012], with increased (decreased) transport of AL relating to salinification
71 (freshening) of AAIW. AL has apparently increased during period from 1950s to the early 21s
72 [Durgadoo *et al.*, 2013; Lübbecke *et al.*, 2015], but no one has focused on discussing the
73 influence of AL on the AAIW in South Atlantic since 2000, especially for the last decade.

74 With the development of Argo (Array for Real-time Geostrophic Oceanography)
75 program, in-situ hydrographic observation has tremendously expanded since 2003 [Roemmich
76 *et al.*, 2015], particularly in the Southern Ocean (SO) where historical data are sparse and
77 intermittent. This decreases the uncertainty for the research on decadal variation of subsurface
78 and intermediate waters.

79 The present work discovers the freshening of AAIW in the South Atlantic for the recent
80 decade (2005 - 2014). Against the background of enhanced hydrological cycle, decreased
81 transport of AL contributes to such a variation, suggested by the weakening of wind stress in
82 the South Indian Ocean during the same period.

83 2. Data and Method

84 Based on individual temperature (T) and salinity (S) profiles from Argo, International
85 Pacific Research Centre (IPRC) gridded monthly means data for period 2005 - 2014 are
86 produced using variational interpolation. The IPRC data have 27 levels from 0 to 2000 m



87 depth vertically, nominal $1^\circ \times 1^\circ$ grid globally and monthly temporal resolution.
88 (http://apdrc.soest.hawaii.edu/projects/Argo/data/gridded/On_standard_levels/index-1.html).
89 To reduce the error from low vertical resolution of data when computing the hydrographic
90 values on isopycnal surface, here T and S profiles are first interpolated onto 1 m interval
91 vertically using spline instead of linear method. Because the IPRC data are interpolated from
92 randomly distributed Argo profiles, it is necessary to demonstrate the robust nature of its
93 signals, by comparing with the other Argo gridded products. As a result, the Japan Agency of
94 Marine-Earth Science and Technology (JAMSTEC, [Hosoda *et al.*, 2008]) T and S data from
95 2005 to 2014 with 1° longitude and 1° latitude resolution are also collected for comparison
96 and verification. The number of Argo profile is rapidly increasing year by year, and part of its
97 distribution had been outlined in some previous studies [Hosoda *et al.*, 2008; Roemmich *et al.*,
98 2015].

99 Two hydrographic occupations of repeated transect along 30° S are collected in the
100 World Ocean Circulation Experiment (WOCE) Hydrographic Program
101 (http://www.nodc.noaa.gov/woce/wdiu/diu_summaries/whp/index.htm). Their positions are
102 presented in Fig. 2. The first occupation was collected with 72 stations in 2003 by the R/V
103 Mirai (Japan, [Kawano *et al.*, 2004]), the other was in 2011 with 81 stations by the Ronald H.
104 Brown (United States, [Feely *et al.*, 2011])
105 (http://www.nodc.noaa.gov/woce/wdiu/diu_summaries/whp/index.htm). These two sections
106 are not only measured in almost the repeated positions in the subtropical South Atlantic, but
107 also performed in the same season (Nov and Oct). Furthermore, the investigation time interval
108 between the two synoptic sections from Nov 2003 to Oct 2011 are nearly the same as the
109 IPRC data (Jan 2005 - Dec 2014), which can be used to confirm the result of IPRC data.

110 To reduce the effect of dynamic process in ocean interior (i.e. mesoscale eddies and
111 internal waves), the investigation of halocline variation would be along neutral density
112 surface [G McCarthy *et al.*, 2011; McDougall, 1987]. The layer of AAIW is defined using
113 neutral density (γ^n , unit: kg/m^3) [Jackett and McDougall, 1997] instead of potential density,
114 with the upper and lower boundaries of $27.1\gamma^n$ and $27.6\gamma^n$ [Goes *et al.*, 2014], respectively.



115 Monthly 10m wind fields between years 1980 and 2014 from ERA-interim archive at
116 European Centre for Medium Range Weather Forecasts (ECMWF)
117 (<http://apps.ecmwf.int/datasets/data/interim-full-daily/levtype=sfc/>) are used to display the
118 decadal variability of wind stress (WS) over the South Indian Ocean. Another reanalysis wind
119 product of NCEP2 (National Centers for Environmental Prediction-Department of Energy
120 Atmospheric Model Intercomparison Project reanalysis 2, NCEP-DOE AMIP Reanalysis-2,
121 <http://www.esrl.noaa.gov/psd/data/gridded/data.ncep.reanalysis2.html>) for period 1980-2014,
122 meanwhile the satellite-derived wind products of QuikSCAT for 2000-2007 and ASCAT for
123 2008-2014 (Quick Scatterometer and Advanced Scatterometer, both in
124 <ftp://ftp.ifremer.fr/ifremer/cersat/products/gridded/MWF/L3/>) are further collected to compare
125 and verify the decadal variability of WS revealed by ERA-interim wind product. The WS in
126 this work over open ocean is calculated from 10 m wind field data using equation adopted in
127 *Trenberth et al.* [1989].

128 Reanalysis data including precipitation (P) and evaporation (E) from ERA-interim are
129 used to reveal the freshwater input from atmosphere to ocean surface in the recent decade.

130 **3. Freshening of Antarctic Intermediate Water**

131 **3.1 Freshening observed from Argo gridded products**

132 The Argo gridded products provide global distributed and continuous time series of T
133 and S profiles down to 2000 m ocean depth. The present work would focus on the AAIW in
134 South Atlantic Basin (Fig. 2, Region A), which encompasses most of the subtropical gyre and
135 a part of the tropical regimes [*Boebel et al.*, 1997; *Talley*, 1996]. By the Argo gridded data of
136 IPRC, the biennial mean of θ - S diagram (Fig. 3a) clearly exhibits that the AAIW has
137 experienced a process of progressively basin-scale freshening during the period from Jan
138 2005 to Dec 2014. The linear trend of salinity (Fig. 3b) further reveals that the freshening
139 takes up most of the AAIW layer but with a little salinification in the lower part of it. Except
140 around the $27.42\gamma^n$ neutral density surface, the AAIW variation is significant at 95%
141 confidence level, using the F -test criteria. In comparison with Fig. 3a, we found that the
142 cut-off point of transformation from salinity decrease to increase is near the salinity minimum.
143 Above salinity minimum, the shift of θ - S curves towards cooler and fresher values along



144 density surface responses to the warming and freshening of surface waters where AAIW
145 ventilates. Such thermohaline change had also been found in the Pacific and Indian oceans
146 over a different time period [Wong *et al.*, 1999], and had been explained by Bindoff and
147 Mcdougall [1994], especially for the counterintuitive cooling of AAIW temperature. For the
148 salinity decline of core of AAIW, it indicates that such change can only be induced by
149 freshwater input from the source region, as mixing with surrounding more saline waters
150 cannot give rise to salt loss in salinity minimum.

151 To demonstrate the robustness of AAIW variations revealed by IPRC data, re-plots of
152 Fig. 3a-b using another Argo gridded product, the JAMSTEC, are also shown for comparison
153 (see Supplementary 1, only AAIW layer shown). Not only the same variation along density
154 surface in the AAIW layer found, but also for the freshening of salinity minimum. Both the
155 isoneutral salinity increases of IPRC and JAMSTEC below salinity minimum are quite small.
156 The most distinct discrepancy between them is that the amplitude of freshening revealed by
157 JAMSTEC is somewhat less than IPRC and at larger 95% confidence level.

158 The freshwater gain for the basin-scale salinity decrease of AAIW (mean salinity
159 difference of 0.012 between 27.1 γ^n and 27.6 γ^n over a mean water mass thickness of 500 m) is
160 estimated at 15mm yr⁻¹ in its source region. However, the depth-integrated salinity change
161 over the water column (between 26.6 γ^n and 27.6 γ^n) is in turn 0.0014, as salinity increase of
162 thermocline water balances the entirely observed freshening of AAIW. This salinity budget
163 implies contemporaneous hydrological cycle intensification in the southern hemisphere,
164 which is illustrated by the *P* less *E* change from 2000 to 2014, with *P-E* increasing in the
165 subpolar region and vice versa in the subtropical region (Fig. 4a). In this case the thermocline
166 (intermediate) water that ventilates in the high-evaporation (precipitation) subtropical
167 (subpolar) regions gets saline (freshened), as shown by the hydrographic observations (Fig.
168 3b).

169 Against the background of hydrological cycle augment, the annually freshwater input in
170 AAIW ventilation region during the freshened period increased by 0.02 mm day⁻¹, about 17%
171 of the *P-E* in 2005 (Fig. 4b). Actually, the increase of *P-E* began in 1992, but significant
172 increase around 2003 (Fig. 4b, 5-yr running mean line), which means the observed freshened



173 AAIW could be traced back to 2003. Though we could not compute the direct freshwater
174 input to the South Atlantic Basin here, the Argo era freshening of AAIW is qualitatively
175 consistent with the freshwater gain in its source region.

176 3.2 Freshening in the quasi-synchronous WOCE CTD observations

177 Here we further used two synoptic transatlantic sections from WOCE hydrographic
178 program to explore the decadal freshened signal in the above subsection. Similar to Fig. 3a,
179 sectional mean θ - S diagram (Fig. 5a) displays a same shift of thermohaline values, including
180 the freshening of salinity minimum, the salinity reduction in upper AAIW layer and vice
181 versa in lower layer. Comparing to the θ - S curves of IPRC data (Fig. 3a), the curves of
182 WOCE (Fig. 5a) seem to be with cooler θ and fresher S in general, this is because the IPRC
183 mean has more weight of warmer and saltier waters in the north.

184 Unlike the Argo gridded product which has continuous time series of T and S data, there
185 are only two sections of snapshot in the WOCE observations. Instead of calculating the linear
186 trend of salinity as the IPRC data done, difference of salinity observed in 2003 and 2011 is
187 estimated (Fig. 5b). The light gray shading denotes the 95% confidence intervals using simple
188 t -test criteria, after considering the number of degrees of freedom. Above the salinity
189 minimum, the freshening of AAIW revealed by IPRC and WOCE data are quite similar, with
190 the maximum appearing near $27.2\gamma^n$. Because the last WOCE observation terminated in 2011
191 and the salinity reduction would continue at least up to 2014 as displayed in Fig. 3a, the
192 magnitude of the freshening in WOCE (Fig. 5b) is a little lesser than IPRC (Fig. 3b). Below
193 the salinity minimum, the salinity increase is relatively large revealed by WOCE data (Fig.
194 3d). This is because the salinity rise reached to its maximum around 2011, shown in the time
195 series of basinwide averaged salinity on $27.45\gamma^n$ and $27.55\gamma^n$ density surfaces (see
196 Supplementary 2).

197 For the salinification of thermocline water, there is a large discrepancy between IPRC
198 and WOCE data, on neutral density surfaces 26.6 - $26.7\gamma^n$ (Fig. 5b). But this would not affect
199 the result that salinity budget over the water column (Fig. 5b), with the salt gain of
200 thermocline water balancing the observed freshened AAIW. In conclusion, the general and
201 detailed consistency of salinity change signal over the last ten year time period revealed by



202 IPRC and WOCE data makes sure that our reported freshening of AAIW is robust and
203 validated.

204 **4. Decrease of Agulhas Leakage transport**

205 AAIW in the South Atlantic is largely influenced by AL through the intermittent
206 pinching off of Agulhas rings (Fig. 2) [Beal *et al.*, 2011], transferring salty thermocline and
207 intermediate water from Indian Ocean to the South Atlantic [De Ruijter *et al.*, 1999]. The
208 above discussion suggests that the freshening of AAIW is induced by input of freshwater
209 from the source region. As a result, if the transport of more saline water from Indian Ocean
210 decreased, it would promote the effect of this freshwater supplement. In this part of paper, the
211 decrease of AL transport would be demonstrated by using an indirect indicator as below. And
212 at last, thorough discussion with respect to other works is displayed.

213 **4.1 Weakening of the westerlies in the South Indian Ocean**

214 There have never been continuous measurements of the AL transport until now. The
215 earlier study suggested that an increased AL transport correlates well with poleward shift of
216 westerlies [Beal *et al.*, 2011]. However, after using reanalysis and climate models, Swart and
217 Fyfe [2012] argued that strengthening of Southern Hemisphere surface westerlies has
218 occurred without robust trend in its latitudinal position over the period from 1979-2010,
219 during which period the AL has largely increased [Bjastoch *et al.*, 2009]. A more recent study
220 of Durgadoo *et al.* [2013] even showed that the increase of AL is concomitant with
221 equatorward rather than poleward shift of westerlies in their simulation cases. And they
222 concluded that the intensity of westerlies is predominantly responsible in controlling this
223 Indian-Atlantic transport. Many relevant studies agreed on this relationship that the
224 enhancement of westerlies intensity relating to the increase of AL [Goes *et al.*, 2014; Lee *et*
225 *al.*, 2011; Loveday *et al.*, 2015].

226 The AL corresponds most significantly to westerlies strength averaged over the Indian
227 Ocean in contrast to that averaged circumpolarly or locally [Durgadoo *et al.*, 2013]. And
228 according to the work of Durgadoo *et al.* [2013], zonally averaged WS was calculated from
229 the wind product of ERA-interim over the Indian Ocean (20-110 °E) for every 5-yr since
230 1980 (Fig. 6a and d). As the same results as many other studies [Lee *et al.*, 2011; Loveday *et*



231 *al.*, 2015], the WS has considerably increased from 1980s to the beginning of 2000s (Fig. 6d),
232 consistent with the contemporaneous increase of AL transport. Though there are oscillations
233 during 1990s, the WS reached to its peak around the years 00-04 (Fig. 6d). And then the WS
234 began to decline. Thus it shows that the WS has weakened for period 2000 – 2014 (Fig. 6d),
235 suggesting the concurrent decrease of AL transport.

236 In addition to the ERA-interim wind data, we have further checked the zonally averaged
237 WS over the Indian Ocean (20-110°E), using another reanalysis product of NCEP2 (Fig. 6b
238 and e) and the combined QuikSCAT-ASCAT (Fig. 6c and f) satellite-derived wind products.
239 All of the three zonally averaged WS agree on that during the period 2000-2014, the
240 westerlies reached to its peak in the years 00-04, and then progressively subsided through
241 05-09 to 10-14. The process of gradual decline of WS is most distinctly illustrated in the
242 NCEP2 data. And what is important, we also note that neither of the three products show a
243 significant meridional shift of the latitude of maximum WS from 2000 to 2014, concomitant
244 with the conclusion of *Swart and Fyfe* [2012].

245 **4.2 Evidence from other works**

246 Many efforts have been made to estimate AL transport, especially using model
247 simulations [*Libbeke et al.*, 2015; *Loveday et al.*, 2015]. In recent years, *Le Bars et al.* [2014]
248 provided the time series of AL transport over the satellite altimeter era, computed from
249 absolute dynamic topography data, which can manifest the decadal variation of AL present
250 here. In their result (Figure 8 in *Le Bars et al.* [2014]), the anomalies of AL from satellite
251 altimeter reached to the peak around 2003 (annual average), and then began to subside,
252 though in the middle of 2011 it appeared to increase again. In addition, their negative trend of
253 AL (Figure 9 in *Le Bars et al.* [2014]) over the period from Oct 1992 to Dec 2012 indicates
254 that the transport reduced during the 2000s in contrast to the 1990s. There is another work
255 done by *Biastoch et al.* [2015] which could support the discussion here. Though the time
256 series of AL obtained from models didn't show a distinct decline of AL transport in the last
257 decade, partly due to the data filter applied and the end of time series in 2010 (Figure 4 in
258 *Biastoch et al.* [2015]), it apparently displays a maximum of salt transport around 2000



259 (Figure 5 in *Biastoch et al.* [2015]). These peak and subsequent decline of salt transport are
260 consistent with the freshening of AAIW over the similar time period observed here.

261 Thus, in addition to the freshwater input that gives rise to the salt loss of the AAIW in
262 South Atlantic Ocean, less transport of AL or salt further facilitate this signal. But
263 unfortunately, both the analysis of contribution from source region and AL are qualitatively
264 instead of quantitatively, only by using the traditionally hydrographic and atmospheric
265 reanalysis data. Future work should be focused on quantification of each factor based on
266 model simulations.

267 5. Conclusions

268 The analysis of IPRC gridded data shows that AAIW in the South Atlantic has
269 experienced basin-scale freshening for the period from Jan 2005 to Dec 2014 (Fig. 3a and b),
270 with freshwater input estimated at 15 mm yr^{-1} in its source region. Two synoptic transects of
271 WOCE hydrographic program observed in 2003 and 2011 also reveal the above well-marked
272 variation of AAIW in the last decade (Fig. 3c and d).

273 Such freshened signal in the intermediate water layer is illustrated to be compensated by
274 increased salinity in shallower thermocline water, indicating the contemporaneous
275 intensification of hydrological cycle (Fig. 3b and Fig. 5b). In this case the freshwater input
276 from atmosphere to ocean surface increased in subpolar high-evaporation region and vice
277 versa in the subtropical high-precipitation region (Fig. 4a). Over the last ten year time period,
278 significant freshwater gain began around 2003 (Fig. 4b), suggesting the observed freshened
279 AAIW could be traced back to this time.

280 Against the background of hydrological intensification, the decrease of AL transport is
281 proposed to contribute to the freshening of AAIW in the South Atlantic, reflected by the
282 weakening of westerlies over South Indian Ocean. It shows that the WS over South Indian
283 Ocean reached to its peak around 00-04 and began to subside through 05-09 to 10-14 (Fig. 6),
284 reversing its increasing phase from 1950s to the beginning of 2000s, during which period the
285 AL had concomitantly increased [*Durgadoo et al.*, 2013; *Libbeke et al.*, 2015]. This
286 indirectly estimated variability of AL, is consistent with the discussion of it over the similar
287 period [*Biastoch et al.*, 2015; *Le Bars et al.*, 2014]. As the AAIW carried by AL is more



288 saline relative to its counterpart in the South Atlantic Ocean, its decrease would promote the
289 effect of freshwater input from the source region, contributing to the observed freshening.

290 Both the analysis of freshwater input and less transport of AL reported here are
291 qualitative but not quantitative. The purpose of this work is to reveal the decadal freshening
292 of AAIW in South Atlantic Ocean over the last ten year time period, and its corresponding
293 mechanism. Future work should be focused on the quantification of these two contributors,
294 meanwhile revealing its influence on the world ocean circulation.

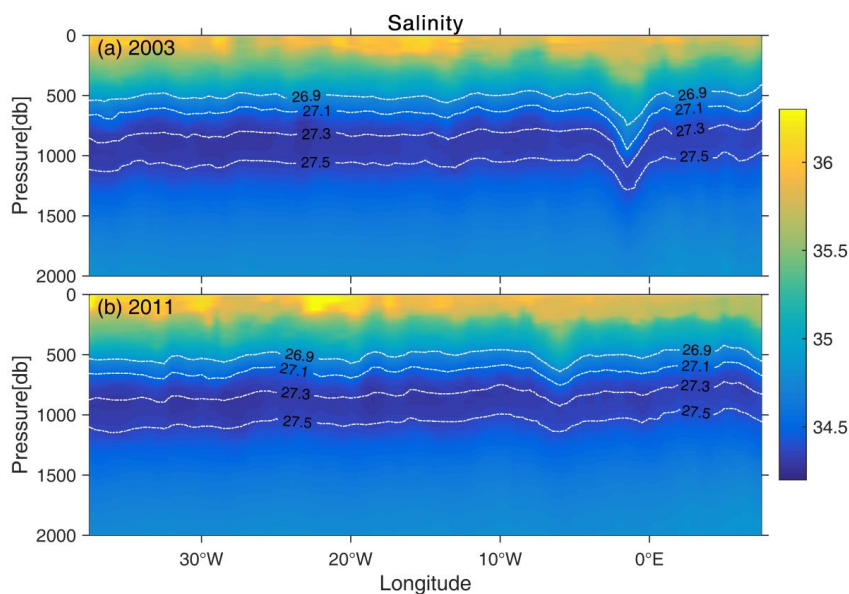
295

296 Acknowledgements

297 This study is supported by the Chinese Polar Environment Comprehensive Investigation
298 and Assessment Programs (Grant nos. CHINARE-04-04, CHINARE-04-01).

299

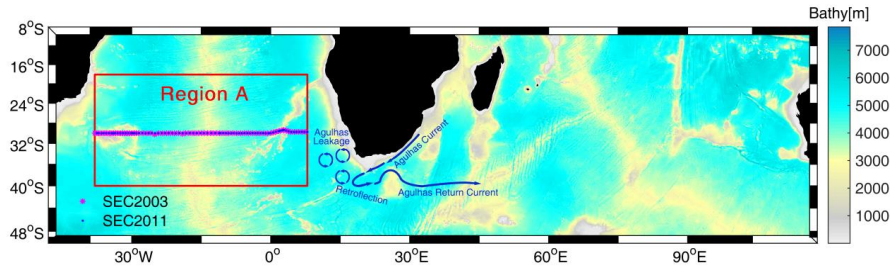
300 Captions of Figures



301

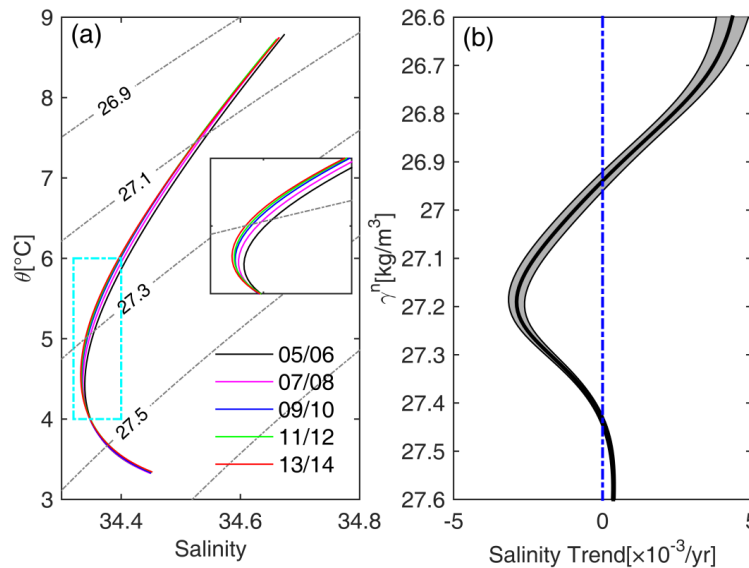
302 Figure 1. WOCE salinity sections along 30°S in the South Atlantic Ocean (positions shown
303 in Fig. 2) observed in (a) 2003 and (b) 2011. Overlaid white solid-dotted lines are σ_{θ} surfaces
304 ranging from 26.9 to 27.5 kg/m³, with 0.2 kg/m³ interval.

305



306

307 Figure 2. Bathymetry of the South Indian-Atlantic oceans. Color shading is ocean depth. Red
 308 box delineates the area for the basinwide average of gridded data (hereafter refers to Region
 309 A). Magenta stars represent transatlantic CTD stations measured in 2003, meanwhile blue
 310 dots in 2011. The Agulhas Current, Retroflexion, Agulhas Return Current and Agulhas
 311 Leakage (as eddies) are also shown and ticked.
 312



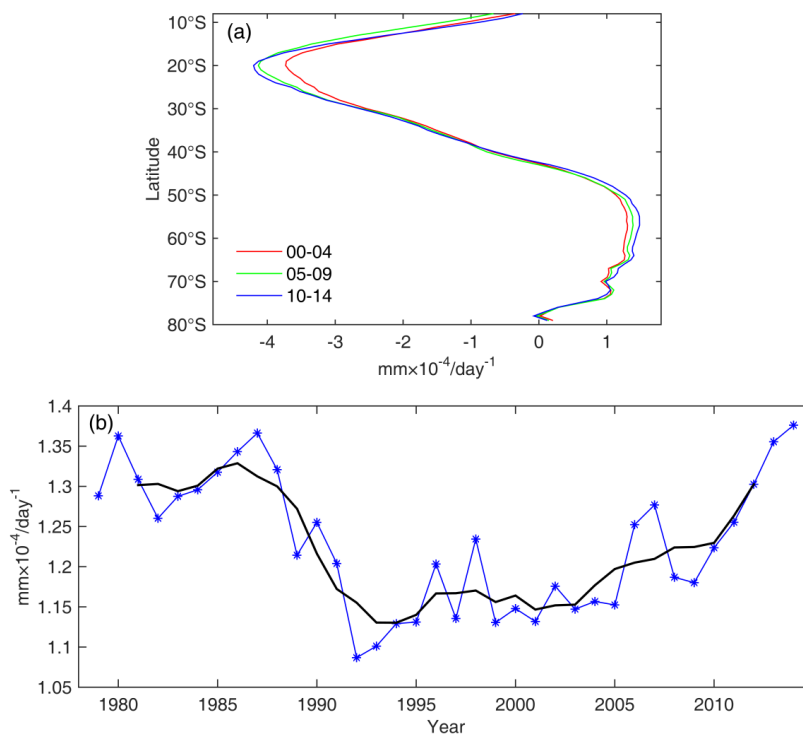
313

314 Figure 3. (a) Biennial mean θ - S diagram averaged over Region A for IPRC data with γ^σ
 315 surfaces superimposed (gray solid-dotted lines). The inserted figure is the magnification of
 316 the area delineated by cyan solid-dotted box. The corresponding time for each θ - S curve in is
 317 listed in their bottom-right corner (i.e. 05/06 for 2005-2006). (b) Salinity trend along γ^σ
 318 surfaces for period Jan 2005 – Dec 2014 is displayed by the thick black line, and the 95%
 319 confidence intervals (F -test) are represented by the light gray shadings, calculated from IPRC
 320 data.
 321

322

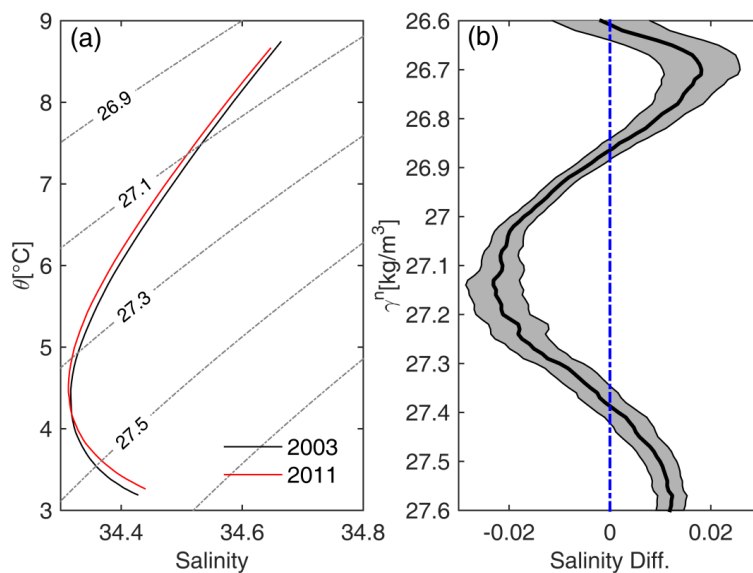


323

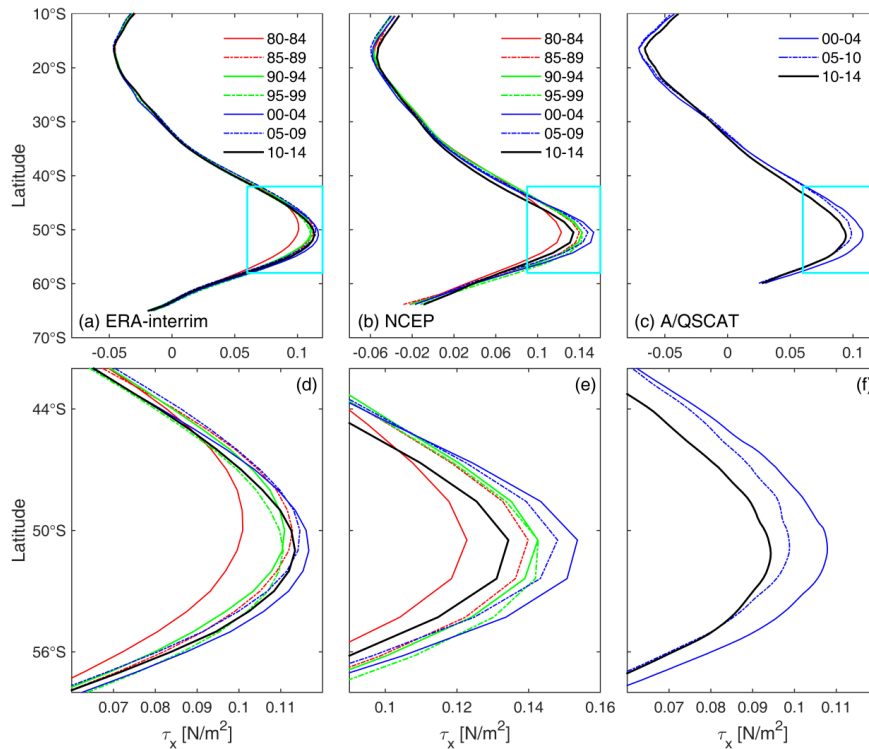


324

325 Figure 4. Calculated from ERA-interim precipitation and evaporation data: (a) Zonally mean
326 (ocean areas only) of annually $P-E$ (freshwater input, mm day^{-1}), each line represents a 5-yr
327 averaged result. The corresponding time period (i.e. 00-04 for 2000-2004) is listed in the
328 bottom-left corner. (b) Time series of annually $P-E$ averaged over the oceans in $45-65^\circ \text{S}$,
329 $0-360^\circ \text{E}$ band from 1979 to 2014 (blue star), and its 5-yr running mean (black).
330



331
332 Figure 5. (a) The same as Fig. 3a but for sectional mean of WOCE hydrographic casts. The
333 corresponding year for each θ - S curve in is listed in their bottom-right corner. (b) Sectional
334 mean differences (thick black line) of WOCE hydrographic data along σ_t and their 95%
335 confidence intervals (gray shadings, t -test).
336



337

338 Figure 6. Zonally averaged wind stress calculated from the wind product of (a) ERA-interim,
 339 (b) NCEP2 and (c) ASCAT/QSCAT over the Indian Ocean (20° E-110° E) for different
 340 periods (i.e. 80-84 for Jan 1980 - Dec 1984; 00-04 for Jan 2000 - Dec 2004) listed in the
 341 top-right corners. (d), (e) and (f) are the magnification of cyan boxes in (a), (b) and (c),
 342 respectively.

343

344 REFERENCES

345 Beal, L. M., W. P. De Ruijter, A. Biastoch, and R. Zahn (2011), On the role of the Agulhas
 346 system in ocean circulation and climate, *Nature.*, 472(7344), 429-436.
 347 Biastoch, A., C. W. Böning, F. U. Schwarzkopf, and J. Lutjeharms (2009), Increase in
 348 Agulhas leakage due to poleward shift of Southern Hemisphere westerlies, *Nature.*,
 349 462(7272), 495-498.
 350 Biastoch, A., J. V. Durgadoo, A. K. Morrison, E. van Sebille, W. Weijer, and S. M. Griffies
 351 (2015), Atlantic multi-decadal oscillation covaries with Agulhas leakage, *Nature*
 352 *communications*, 6.
 353 Bindoff, N. L., and T. J. McDougall (1994), Diagnosing climate change and ocean ventilation
 354 using hydrographic data, *J. Phys. Oceanogr.*, 24(6), 1137-1152.
 355 Bindoff, N. L., and T. J. McDougall (2000), Decadal changes along an Indian Ocean section
 356 at 32° S and their interpretation, *J. Phys. Oceanogr.*, 30(6), 1207-1222.



- 357 Boebel, O., C. Schmid, and W. Zenk (1997), Flow and recirculation of Antarctic intermediate
358 water across the Rio Grande rise, *J. Geophys. Res. Oceans (1978–2012)*, *102(C9)*,
359 20967-20986.
- 360 Church, J. A., J. S. Godfrey, D. R. Jackett, and T. J. McDougall (1991), A model of sea level
361 rise caused by ocean thermal expansion, *J. Climate.*, *4(4)*, 438-456.
- 362 Close, S. E., A. C. Naveira Garabato, E. L. McDonagh, B. A. King, M. Biuw, and L. Boehme
363 (2013), Control of mode and intermediate water mass properties in Drake Passage by the
364 Amundsen Sea Low, *J. Climate.*, *26(14)*, 5102-5123.
- 365 Curry, R., B. Dickson, and I. Yashayaev (2003), A change in the freshwater balance of the
366 Atlantic Ocean over the past four decades, *Nature.*, *426(6968)*, 826-829.
- 367 De Ruijter, W., A. Biastoch, S. Drijfhout, J. Lutjeharms, R. Matano, T. Pichevin, P. Van
368 Leeuwen, and W. Weiger (1999), Indian-Atlantic interocean exchange: Dynamics, estimation
369 and impact, *J. Geophys. Res.*, *104(C9)*, 20885-20910.
- 370 Donners, J., and S. S. Drijfhout (2004), The Lagrangian view of South Atlantic interocean
371 exchange in a global ocean model compared with inverse model results, *J. Phys. Oceanogr.*,
372 *34(5)*, 1019-1035.
- 373 Durgadoo, J. V., B. R. Loveday, C. J. C. Reason, P. Penven, and A. Biastoch (2013), Agulhas
374 Leakage Predominantly Responds to the Southern Hemisphere Westerlies, *J. Phys. Oceanogr.*,
375 *43(10)*, 2113-2131.
- 376 Feely, R. A., R. Wanninkhof, S. Alin, M. Baringer, and J. Bullister (2011), Global Repeat
377 Hydrographic/CO₂/Tracer surveys in Support of CLIVAR and Global Cycle objectives:
378 Carbon Inventories and Fluxes.
- 379 Fetter, A., M. Schodlok, and V. Zlotnicki (2010), Antarctic Intermediate Water Formation in a
380 High-Resolution OGCM, paper presented at EGU General Assembly Conference Abstracts.
- 381 Goes, M., I. Wainer, and N. Signorelli (2014), Investigation of the causes of historical
382 changes in the subsurface salinity minimum of the South Atlantic, *J. Geophys. Res. Oceans*,
383 *119(9)*, 5654-5675.
- 384 Gordon, A. L., R. Weiss, W. M. Smethie Jr, and M. J. Warner (1992), Thermocline and
385 Intermediate Water Communication, *J. Geophys. Res.*, *97(C5)*, 7223-7240.
- 386 Held, I. M., and B. J. Soden (2006), Robust responses of the hydrological cycle to global
387 warming, *J. Climate.*, *19(21)*, 5686-5699.
- 388 Hosoda, S., T. Ohira, and T. Nakamura (2008), A monthly mean dataset of global oceanic
389 temperature and salinity derived from Argo float observations, *JAMSTEC Rep. Res. Dev.*, *8*,
390 47-59.
- 391 Hummels, R., P. Brandt, M. Dengler, J. Fischer, M. Araujo, D. Veleda, and J. V. Durgadoo
392 (2015), Interannual to decadal changes in the western boundary circulation in the Atlantic at
393 11 °S, *Geophys. Res. Lett.*, *42(18)*, 7615-7622.
- 394 Jackett, D. R., and T. J. McDougall (1997), A neutral density variable for the world's oceans, *J.*
395 *Phys. Oceanogr.*, *27(2)*, 237-263.
- 396 Kawano, T., H. Uchida, W. Schneider, Y. Kumamoto, A. Nishina, M. Aoyama, A. Murata, K.
397 Sasaki, Y. Yoshikawa, and S. Watanabe (2004), Cruise Summary of WHP P6, A10, I3 and I4
398 Revisits in 2003, paper presented at AGU Fall Meeting Abstracts.
- 399 Lübbecke, J. F., J. V. Durgadoo, and A. Biastoch (2015), Contribution of increased Agulhas



- 400 leakage to tropical Atlantic warming, *J. Climate.*, 28(24), 9697-9706.
- 401 Le Bars, D., J. V. Durgadoo, H. A. Dijkstra, A. Biastoch, and W. P. M. De Ruijter (2014), An
402 observed 20-year time series of Agulhas leakage, *Ocean Sci.*, 10(4), 601-609.
- 403 Lee, S. K., W. Park, E. van Sebille, M. O. Baringer, C. Wang, D. B. Enfield, S. G. Yeager, and
404 B. P. Kirtman (2011), What caused the significant increase in Atlantic Ocean heat content
405 since the mid - 20th century?, *Geophys. Res. Lett.*, 38(17).
- 406 Loveday, B., P. Penven, and C. Reason (2015), Southern Annular Mode and westerly -
407 wind - driven changes in Indian - Atlantic exchange mechanisms, *Geophys. Res. Lett.*, 42(12),
408 4912-4921.
- 409 McCarthy, G., E. McDonagh, and B. King (2011), Decadal variability of thermocline and
410 intermediate waters at 24 S in the South Atlantic, *J. Phys. Oceanogr.*, 41(1), 157-165.
- 411 McCarthy, G. D., B. A. King, P. Cipollini, E. L. McDonagh, J. R. Blundell, and A. Biastoch
412 (2012), On the sub-decadal variability of South Atlantic Antarctic Intermediate Water,
413 *Geophys. Res. Lett.*, 39, L10605.
- 414 McCartney, M. S. (1977), Subantarctic Mode Water, in *Angel, M.V. (Ed.), A Voyage of*
415 *Discovery: George Deacon 70th Anniversary Volume (Suppl. To Deep-Sea Res.)*, Pergamon,
416 edited, pp. 103-119, Woods Hole Oceanographic Institution.
- 417 McCartney, M. S. (1982), The subtropical recirculation of mode waters, *J. Mar. Res.*, 40,
418 427-464.
- 419 McDougall, T. J. (1987), Neutral surfaces, *J. Phys. Oceanogr.*, 17(11), 1950-1964.
- 420 Naveira Garabato, A. C., L. Jullion, D. P. Stevens, K. J. Heywood, and B. A. King (2009),
421 Variability of Subantarctic Mode Water and Antarctic Intermediate Water in the Drake
422 Passage during the Late-Twentieth and Early-Twenty-First Centuries, *J. Climate.*, 22(13),
423 3661-3688.
- 424 Orsi, A. H., T. Whitworth Iii, and W. D. Nowlin Jr (1995), On the meridional extent and fronts
425 of the Antarctic Circumpolar Current, *Deep-Sea Res. I.*, 42(5), 641-673.
- 426 Piola, A. R., and D. T. Georgi (1982), Circumpolar properties of Antarctic intermediate water
427 and Subantarctic Mode Water, *Deep-Sea Res. A.*, 29(6), 687-711.
- 428 Ridgway, K. R., and J. R. Dunn (2007), Observational evidence for a Southern Hemisphere
429 oceanic supergyre, *Geophys. Res. Lett.*, 34, L13612.
- 430 Roemmich, D., J. Church, J. Gilson, D. Monselesan, P. Sutton, and S. Wijffels (2015),
431 Unabated planetary warming and its ocean structure since 2006, *Nature Clim. Change*, 5(3),
432 240-245.
- 433 Santoso, A., and M. H. England (2004), Antarctic Intermediate Water circulation and
434 variability in a coupled climate model, *J. Phys. Oceanogr.*, 34(10), 2160-2179.
- 435 Schmidtko, S., and G. C. Johnson (2012), Multidecadal Warming and Shoaling of Antarctic
436 Intermediate Water*, *J. Climate.*, 25(1), 207-221.
- 437 Skliris, N., R. Marsh, S. A. Josey, S. A. Good, C. Liu, and R. P. Allan (2014), Salinity changes
438 in the World Ocean since 1950 in relation to changing surface freshwater fluxes, *Climate*
439 *dynamics*, 43(3-4), 709-736.
- 440 Sloyan, B. M., and S. R. Rintoul (2001), Circulation, Renewal, and Modification of Antarctic
441 Mode and Intermediate Water*, *J. Phys. Oceanogr.*, 31(4), 1005-1030.
- 442 Speich, S., B. Blanke, and W. Cai (2007), Atlantic meridional overturning circulation and the



- 443 Southern Hemisphere supergyre, *Geophys. Res. Lett.*, *34*, L23614.
444 Speich, S., B. Blanke, P. de Vries, S. Drijfhout, K. Döös, A. Ganachaud, and R. Marsh (2002),
445 Tasman leakage: A new route in the global ocean conveyor belt, *Geophys. Res. Lett.*, *29*(10),
446 1416.
447 Sun, C., and D. R. Watts (2002), A view of ACC fronts in streamfunction space, *Deep-Sea*
448 *Res. I.*, *49*(7), 1141-1164.
449 Sverdrup, H. U., M. W. Johnson, and R. H. Fleming (1942), *The Oceans: Their physics,*
450 *chemistry, and general biology*, Prentice-Hall New York.
451 Swart, N., and J. Fyfe (2012), Observed and simulated changes in the Southern Hemisphere
452 surface westerly wind - stress, *Geophys. Res. Lett.*, *39*(L16711).
453 Talley, L. D. (1996), Antarctic intermediate water in the South Atlantic, in *The South Atlantic*,
454 edited, pp. 219-238, Springer.
455 Talley, L. D. (2013), Closure of the global overturning circulation through the Indian, Pacific,
456 and Southern Oceans: Schematics and transports, *Oceanography*, *26*(1), 80-97.
457 Trenberth, K. E., W. G. Large, and J. G. Olson (1989), The effective drag coefficient for
458 evaluating wind stress over the oceans, *J. Climate.*, *2*(12), 1507-1516.
459 Wong, A. P., N. L. Bindoff, and J. A. Church (1999), Large-scale freshening of intermediate
460 waters in the Pacific and Indian Oceans, *Nature.*, *400*(6743), 440-443.
461 Wong, A. P., N. L. Bindoff, and J. A. Church (2001), Freshwater and heat changes in the
462 North and South Pacific Oceans between the 1960s and 1985-94, *J. Climate.*, *14*(7),
463 1613-1633.
464
465